

# Minimal model of diffusion with time changing Hurst exponent

Jakub Ślęzak<sup>†</sup> and Ralf Metzler<sup>‡,‡</sup>

<sup>†</sup> Hugo Steinhaus Center, Wrocław University of Science and Technology, Poland

<sup>‡</sup> Institute of Physics & Astronomy, University of Potsdam, Germany

<sup>‡</sup> Asia Pacific Centre for Theoretical Physics, Pohang 37673, Republic of Korea

E-mail: jakub.slezak@pwr.edu.pl, rmetzler@uni-potsdam.de (Corresponding author: Ralf Metzler)

**Abstract.** We introduce the stochastic process of incremental multifractional Brownian motion (IMFBM), which locally behaves like fractional Brownian motion with a given local Hurst exponent and diffusivity. When these parameters change as function of time the process responds to the evolution gradually: only new increments are governed by the new parameters, while still retaining a power-law dependence on the past of the process. We obtain the mean squared displacement and correlations of IMFBM which are given by elementary formulas. We also provide a comparison with simulations and introduce estimation methods for IMFBM. This mathematically simple process is useful in the description of anomalous diffusion dynamics in changing environments, e.g., in viscoelastic systems, or when an actively moving particle changes its degree of persistence or its mobility.

## 1. Introduction and background

The modern study of diffusive processes started at the beginning of the 20th century when Albert Einstein [1], Marian Smoluchowski [2], William Sutherland [3], and Paul Langevin [4] proposed the physical theory of Brownian motions (later formalised by Norbert Wiener [5]), laying the foundations for what is now the theory of stochastic processes and nonequilibrium statistical physics [6–9]. Brownian motion is characterised by a linear mean squared displacement (MSD) and a Gaussian probability density function (PDF) [10,11]. While single particle tracking already was well established in the early experiments of Perrin [12] and Nordlund [13], with modern microscopic techniques the stochastic motion of microscopic particles or even single molecules can now be routinely recorded in complex environments such as living biological cells [14]. Single trajectories are also measured for moving cells, small organism, or even large animals, among many other applications [14–20]. Such experiments demonstrate that in many complex systems the MSD is no longer linear in time but follows the power-law form  $\langle X^2(t) \rangle \propto t^{2H}$ , where the Hurst exponent  $H$  distinguishes subdiffusion ( $0 < H < 1/2$ ) from superdiffusion ( $1/2 < H < 1$ ) [21].

A widely used generalisation of the Einstein-Smoluchowski-Langevin theory of Brownian motion is fractional Brownian motion (FBM)  $B_H(t)$ , the only stochastic process which is Gaussian and exhibits power-law memory between its increments<sup>‡</sup>

$$\left\langle \frac{dB_H(s)}{ds} \frac{dB_H(t)}{dt} \right\rangle = DC_H |t - s|^{2H-2}, \quad C_H \equiv H(2H - 1). \quad (1)$$

Here the parameter  $D$  is the (generalised) diffusion coefficient. Integrating over this formula twice shows that the MSD has the power-law form  $\langle B_H(t)^2 \rangle = Dt^{2H}$ . In this context the coefficient  $D$  can be interpreted as the scale of the process for a given anomalous diffusion exponent  $2H$ . A process closely related to FBM was originally proposed by Kolmogorov [23], and FBM was widely popularised by Benoît Mandelbrot and John van Ness in their seminal paper [24,25]. Mandelbrot and van Ness were in fact inspired not by diffusion, but Harold Hurst's studies of water flows [26], economic cycles, and fractional  $1/f^\alpha$  noises. In line with their interdisciplinary approach, contemporary applications of FBM span very diverse fields, from broadband network traffic [27] to the structure of star clusters [28], and financial market dynamics [29]. Characteristics of subdiffusive FBM were, i.a., observed for the motion of submicron tracers in soft and bio matter [30–36]. Superdiffusive motion consistent with FBM was observed in actively driven motion in biological cells [37,38] and in movement ecology [15,39]. We note that non-Gaussian forms of FBM measured, e.g., in biological cells [40–42], may arise from FBM with randomly fluctuating diffusion coefficient [43–46].

The cases of subdiffusion ( $0 < H < 1/2$ ) and superdiffusion ( $1/2 < H < 1$ ) have differing physical interpretations and are only rarely observed together [36,47]. For  $0 < H < 1/2$  the process exhibits negative memory (see equation (1)), a property referred to as antipersistence. The negative dependence between increments and the covariance integrates to zero,  $\int_{-\infty}^{\infty} \left\langle \frac{dB_H(s)}{ds} \frac{dB_H(s+t)}{dt} \right\rangle dt = 0$ . For  $1/2 < H < 1$  the positive dependence between increments causes the memory to be persistent, featuring a non-integrable tail of the covariance function, such that  $\int_1^{\infty} \left\langle \frac{dB_H(s)}{ds} \frac{dB_H(s+t)}{dt} \right\rangle dt = \infty$  [48]. It is worth adding that FBM is also used as a noise in generalised Langevin equations [49–51].

Definition (1), while uniquely determining FBM and separating it from other anomalous diffusion models, such as non-Gaussian subdiffusive random walks [21], does not provide an explicit construction of the FBM process. This can be achieved with one of the few equivalent integral representations. The Fourier representation, equivalently for the increments and the process itself, reads<sup>§</sup>

$$dB_H(t) = \frac{\sqrt{D}}{\gamma_H} \int_{-\infty}^{\infty} \frac{i\omega e^{i\omega t}}{|\omega|^{H+1/2}} dt dZ(\omega) \quad \text{and} \quad B_H(t) = \frac{\sqrt{D}}{\gamma_H} \int_{-\infty}^{\infty} \frac{e^{i\omega t} - 1}{|\omega|^{H+1/2}} dZ(\omega) \quad (2)$$

<sup>‡</sup> For  $H \leq 1/2$  this expression has a strong singularity at  $t - s = w \rightarrow 0$  which should be carefully accounted for. In integrals it is interpreted as  $\frac{d}{dw}(H|w|^{2H-1} \text{sgn } w)$  [22], similarly to equation (3) below.  
<sup>§</sup> Mathematically interpreted as the stochastic integral over complex-valued white Gaussian noise  $dZ(\omega)$ .

with the rescaling constant  $\gamma_H \equiv \sqrt{2\pi}(\sin(\pi H)\Gamma(2H + 1))^{-1/2}$ . This representation has the advantage of emphasising that FBM is a model for a system at statistical equilibrium. Indeed, shifting time by some  $t_0$  only multiplies the integrand on the left by the complex phase  $\exp(it_0\omega)$  which leads to the same (real valued) PDF due to Gaussian distribution isotropy of the  $dZ$ . It also directly demonstrates that FBM is a  $1/f^\alpha$  process with power spectral density  $|\omega|^{1/2-H}$ . Another representation of FBM is the integral  $\int_{-\infty}^t ((t-s)_+^{H-1/2} - (-s)_+^{H-1/2})dB_s$  with  $(t)_+ \equiv \max(t, 0)$ ; for more details see [52].

The strong symmetries of FBM make its Hurst index the unifying parameter governing both its short and long time properties. This fact restricts some of its applications—crucially for us it makes it impossible to describe an increasing number of regime-switching anomalous diffusion systems in which the anomalous diffusion exponent and the diffusivity change as functions of time. Examples for such phenomena include the motion of a tracer in the changing viscoelastic environment of cells during their cycle [53] or in viscoelastic solutions under pressure and/or concentration changes [54,55], in actin gels with changing mesh size [56], the motion of lipid molecules in cooling bilayer membranes [35], passive and active intracellular movement after treatment with chemicals [37,57], or intra- and inter-daily variations in the movement dynamics of larger animals [58]. Quite abrupt changes of  $H$  and/or  $D$  may be effected by binding to larger objects or surfaces [41, 59] or multimerisation [59, 60] of the tracer.

In order to overcome the limitations of FBM, multifractional Brownian motion (MFBM) models were created, initially motivated by terrain modelling [61]. A process is considered to be an MFBM if it resembles FBM locally, i.e., its increments  $dX(t)$  resemble increments of FBM  $dB_H$  with local parameters, a property called local self similarity [62]. This definition does not specify any global features of the process, such as the dependence between different  $dX(s)$  and  $dX(t)$ —these can vary from model to model. Benassi, Roux and Jaffard proposed an especially useful MFBM defined by substituting  $H \rightarrow \mathcal{H}_t$  into the right hand side of the integral in equation (2) [63]. The simple mathematical form of the Fourier transform allowed Ayache *et al* to calculate the exact distribution of this model, a clear advantage for practical applications; in particular it has MSD  $Dt^{2\mathcal{H}_t}$  [64]. For information about other MFBM variants see, e.g., the 2006 review by Stoev and Taqqu [65]. Recently, a Memory MFBM (MMFBM) model was proposed in order to describe viscoelastic or persistent anomalous diffusion with physically meaningful persistence of correlations [66]. Another very closely related class of processes are linear time series models with fractionally integrated noises (ARFIMA) and time dependent coefficients [67]. Inter alia MFBMs found applications in finance, where it is natural to expect a time-dependence of the market dynamics [68–71], and also network traffic [72], geometry of mountain ranges [73] or atmospheric turbulence [74], as well as heterogeneous diffusion [45]. Statistical methods for analysing MFBM models include wavelet decomposition [75], covariance and MSD analysis and testing [76], or neural networks [77].

In the standard MFBM models the history of the Hurst exponent  $\mathcal{H}_s, s < t$  does

not affect future observed displacements, only the local value of  $\mathcal{H}_t$  matters. This feature does not affect the above-mentioned applications of MFBMs as they are mostly concerned with the local roughness of the observed data, not its global moments and correlations. This "amnesia" of the Hurst exponent is also the reason behind MFBMs' simple mathematical structure. However, it is not a desirable property for modelling diffusion in complex media where an evolving  $\mathcal{H}_t$  should reflect the physical changes in the environment which determine the further evolution of the process due to the inherent long-range memory. The forgetfulness of MFBMs also forces the trajectories to "bend" to an evolving  $\mathcal{H}_t$ : Rapid changes of  $\mathcal{H}_t$  lead to rapid, jump-like changes of the trajectory  $X(t)$ . In physical and biological contexts we would rather expect that—in the same manner as for the diffusivity—changes of  $H$  (even rapid) should lead to a gradual response to a new environment due to the governing long-range memory structure.

In the following we introduce and state the fundamental properties of a minimal model for FBM with a time-evolving Hurst exponent in section 2. We then present concrete results for a step-wise change of the Hurst exponent and the diffusion coefficient in section 3. Finally we discuss our results in a broader context in section 4. Simulation and estimation methods for the model are shown in the Supplementary material.

## 2. Definition of the minimal model

In our approach to establish a minimal model to resolve the question of how we can model anomalous diffusion of the FBM type with long-range correlations and time-evolving transport coefficients  $H$  and  $D$  we want to preserve the simple mathematical structure of the existing MFBM models but modify this structure such that it does not directly affect the position of the particle but reflects the gradual influence on the particle dynamics following environmental changes as mediated by the memory structure of FBM. To this end we consider an FBM-type diffusion for which the change in the environment leads to changes of the Hurst exponent and diffusion coefficient. It is then physically more natural to assume that this will not cause the whole trajectory to "switch" to a new  $H$ , but only affect the new increments after the change. In different words, changes of  $H$  should lead to direct changes of the increments and to only indirect changes of the position.

The simplest way of fulfilling this requirement is to modify the memory structure of FBM to

$$\left\langle \frac{dB_{\mathcal{H}}(s)}{ds} \frac{dB_{\mathcal{H}}(t)}{dt} \right\rangle = \sqrt{\mathcal{D}_s \mathcal{D}_t} C_{\mathcal{H}_s, \mathcal{H}_t} |t - s|^{\mathcal{H}_s + \mathcal{H}_t - 2}, \quad (3)$$

where the rescaling constant  $C_{\mathcal{H}_s, \mathcal{H}_t}$  ( $C_{H, H} = C_H$ ) is to be determined at the end of this section. We also require the process to be Gaussian, as is FBM. Thus, the process (3) is uniquely determined, as there is only one Gaussian variable with a given covariance (and zero mean). The resulting dynamic has a Hurst index defined by the arithmetic mean  $H \rightarrow (\mathcal{H}_s + \mathcal{H}_t)/2$  and a diffusion coefficient given by the geometric mean  $D \rightarrow \sqrt{\mathcal{D}_s \mathcal{D}_t}$ . For any period with constant parameters  $\mathcal{H}_t = H$  and  $\mathcal{D}_t = D$  this process clearly

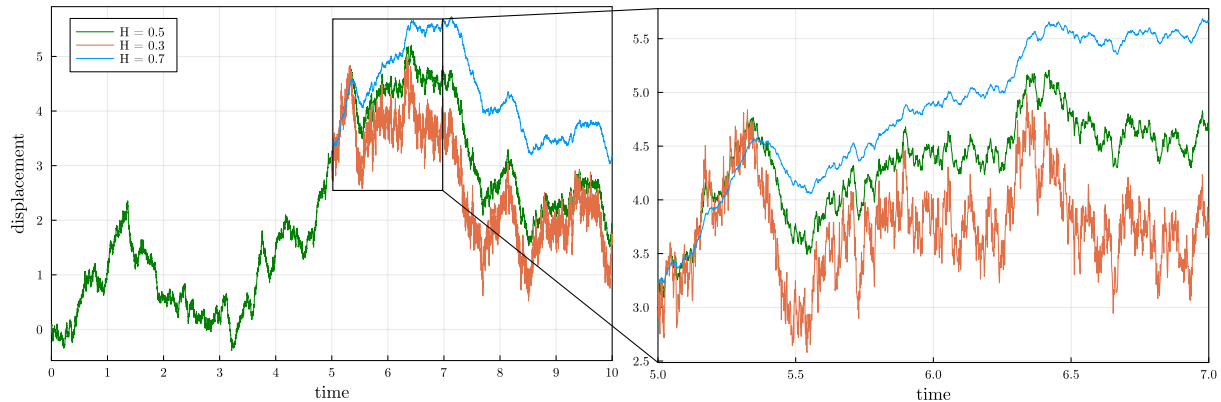


**Figure 1.** Comparison of three trajectories, which represent normal Brownian motion until  $t = 5$  and then switch to subdiffusion, superdiffusion, or stay Brownian. The trajectories are based on the same realisation of the stochastic noise. We see how a low  $H$  ( $< 1/2$ ) introduces antipersistence by amplifying the periods in which the trajectory turns back and, conversely, how high  $H$  ( $> 1/2$ ) introduces a persistence by amplifying excursions in the same direction. The right panel shows a zoom into the part of the trajectory right after the switching of  $H$ . The simulations were performed using our introduced model with time changing  $H$ , the procedure is explained in the Supplementary Material.

reduces to a standard FBM, and thus this process belongs to the broad class of MFBMs. As it is defined through its increments we will call it incremental MFBM (IMFBM). We demonstrate how a changing Hurst exponent affects IMFBM trajectories in figure 1. We note that the trajectory of MFBM would lead to a discontinuity at the point where  $H$  is changing.

Equation (3) completely determines the memory structure of IMFBM. The quantity  $\langle dB_{\mathcal{H}}(s)dB_{\mathcal{H}}(t) \rangle$  can be interpreted as a response function  $r = r(s, t)$ , that determines to which extent any past infinitesimal change  $dB_{\mathcal{H}}(s)$  influences linearly the current change  $dB_{\mathcal{H}}(t)$ : the feedback is negative, i.e.,  $r < 0$ , for  $\mathcal{H}_s + \mathcal{H}_t < 1$  and positive ( $r > 0$ ) for  $\mathcal{H}_s + \mathcal{H}_t > 1$ . A heavy, non-integrable tail of  $r$  is present when  $\mathcal{H}_s + \mathcal{H}_t > 1$ .

Assuming we start our observation at 0,  $B_{\mathcal{H}}(0) = 0$ , the MSD of IMFBM can be obtained from the integral

$$\langle B_{\mathcal{H}}(t)^2 \rangle = \left\langle \left( \int_0^t dB_{\mathcal{H}}(s) \right)^2 \right\rangle = \int_0^t \int_0^t \langle dB_{\mathcal{H}}(s_1)dB_{\mathcal{H}}(s_2) \rangle, \quad (4)$$

where the integrand is given by relation (3). Analogously, to obtain the full covariance  $\langle B_{\mathcal{H}}(s)B_{\mathcal{H}}(t) \rangle$  only the limits of the integrals are changed to  $\int_0^s \int_0^t$ . Note that the result does not depend on the past of  $\mathcal{H}_t, \mathcal{D}_t, t < 0$ . If the evolution of the system initiated at some  $t_0 < 0$  and we started observing it at time  $t = 0$  the measured displacements  $B_{\mathcal{H}}(t) - B_{\mathcal{H}}(0)$  would be the same as in (4). This is a practical feature based on the stationarity, ingrained in (3), of the underlying displacements, due to which IMFBM

|| This formulation is connected to Riemman Liouville FBM as originally formulated by Lévy [24, 78].

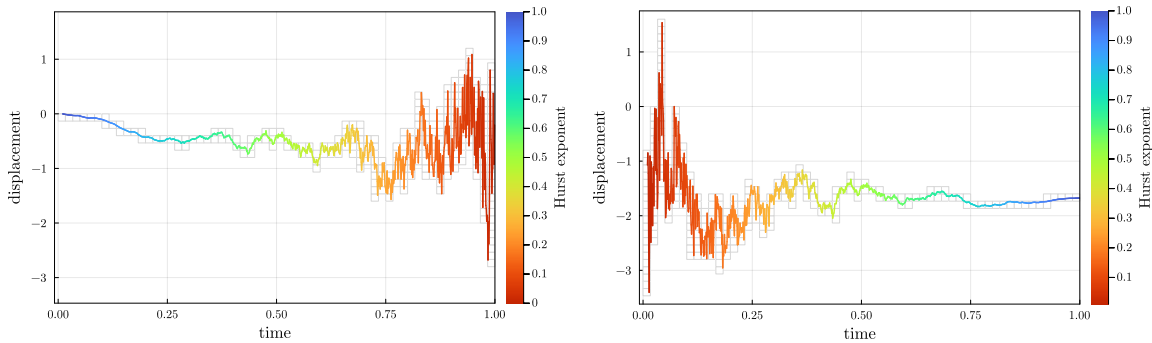


**Figure 2.** Trajectory of IMFBM for which the Hurst exponent decreases linearly from 1 to 0 (left panel) or increases linearly from 0 to 1 (right panel). The grey areas show boxes with fixed size  $\epsilon$ , which cover the trajectory. The more irregular the trajectory is locally, the more it "covers" the space. In the limit  $\epsilon \rightarrow 0$  the number of required boxes locally increases proportionally to the fractal dimension,  $\epsilon^{-(2-\mathcal{H}_t)}$  [82].

depends only on observed quantities.

From equation (4) it is also apparent that in the special case  $\mathcal{H}_t = H = \text{const.}$  and  $\mathcal{D}_t \neq \text{const.}$  the process reduces to

$$B_{\mathcal{H}}(t) = \int_0^t \sqrt{\mathcal{D}_s} dB_H(s), \quad (5)$$

which is a natural choice of extending FBM to incorporate a time-varying diffusivity [66]. When  $\mathcal{H}_t = 1/2$  this integral reduces to scaled Brownian motion, a widely used Markovian model of diffusion with time-evolving diffusivity [79, 80].

The above example shows that the choice of time changing diffusivity  $D \rightarrow \sqrt{\mathcal{D}_s \mathcal{D}_t}$  appears quite natural. The second part of the IMFBM definition, the choice of  $H \rightarrow (\mathcal{H}_s + \mathcal{H}_t)/2$  can be interpreted as imposing a linear dependence on the Hurst exponent history. The current increment  $dB_{\mathcal{H}}$  is correlated with a past increment with a weight proportional to  $|t-s|^{\mathcal{H}_s} ds$ . This relation is linear only for substitutions of the form  $H \rightarrow \lambda \mathcal{H}_s + (1-\lambda)\mathcal{H}_t$  with  $0 \leq \lambda \leq 1$ . Giving equal weight to past and present,  $\lambda = 1/2$ , appears as a reasonable default choice. It also makes sure that trajectories of IMFBM (analogously to other MFBMs) locally resemble FBM with parameters  $\mathcal{D}_t, \mathcal{H}_t$ , thus preserving the local roughness of the trajectory: for smooth changes of  $\mathcal{H}$  and  $\mathcal{D}$  it has local fractal dimension  $2 - \mathcal{H}_t$ ¶, as illustrated in figure 2.

Returning to equation (3), we note that similar to (1) for FBM, it does not provide a representation (a direct construction) of the process. In fact, without such a representation, one cannot even be sure that such a process exists mathematically. Due to its elegant mathematical form the Fourier definition (2) of FBM turns out to be useful here, as well. We simply substitute  $D \rightarrow \mathcal{D}_t$  and  $H \rightarrow \mathcal{H}_t$  into the left integral in

¶ It fulfils the conditions for a fractal dimension given in [81].

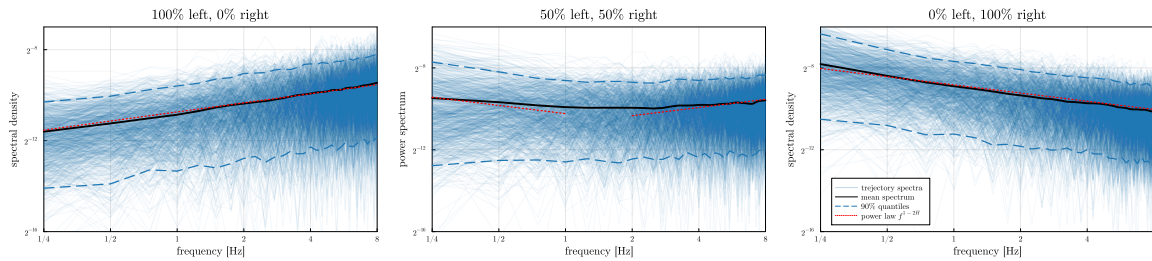


**Figure 3.** Spectral densities calculated from a window of 1000 differentiated IMFBM trajectory realisations with a single change of parameters from  $H_1 = 0.3, D_1 = 1$  to  $H_2 = 0.7, D_2 = 16$  (see also section 3). In the Left panel the window is fully in the range of  $H_1 = 0.3$  and the power law spectrum agrees with the one of classical FBM. In the Right panel, analogously, we see the same for a window fully in the range of  $H_2 = 0.7$ . In the Centre panel we observe a mixed spectrum which on the left side is mostly affected by the subdiffusive  $H_1 = 0.3$  and on the right by the superdiffusive  $H_2 = 0.7$ .

(2) and get<sup>+</sup>

$$dB_{\mathcal{H}}(t) \equiv \frac{\sqrt{\mathcal{D}_t}}{\gamma_{\mathcal{H}_t}} \int_{-\infty}^{\infty} \frac{i\omega e^{i\omega t}}{|\omega|^{\mathcal{H}_t+1/2}} dt dZ(\omega). \quad (6)$$

By construction, this representation makes sure that the process is Gaussian, as a combination of Gaussian increments  $dZ(\omega)$ . For  $\mathcal{H}_t, \mathcal{D}_t \neq \text{const.}$  the process is non-ergodic and non-stationary. Its increments belong to the class of evolutionary spectra processes [83] with power-law time dependent spectrum  $\text{sgn}(\omega)|\omega|^{1-2\mathcal{H}_t}$ , see figure 3. This power-law distribution of the probability mass over frequencies determines the local fractal properties of the process, which are locally like those of regular FBM.

It follows from the linearity of the Fourier transform that the covariance of IFBM fits our requirement (3); essentially this process has the two-point Fourier amplitude  $\propto \sqrt{\mathcal{D}_s \mathcal{D}_t} |\omega|^{1-\mathcal{H}_s-\mathcal{H}_t}$  and it enforces (3). Using relation (6) we can determine the rescaling coefficient  $C_{\mathcal{H}_s, \mathcal{H}_t}$ : this can be achieved using integral tables from which we find  $C_{\mathcal{H}_s, \mathcal{H}_t} = c_{\mathcal{H}_s, \mathcal{H}_t} C_{(\mathcal{H}_s+\mathcal{H}_t)/2}$  with  $c_{\mathcal{H}_s, \mathcal{H}_t} \equiv \gamma_{(\mathcal{H}_s+\mathcal{H}_t)/2}^2 / (\gamma_{\mathcal{H}_s} \gamma_{\mathcal{H}_t})$ . For periods of constant  $H$ ,  $c_{H,H} = 1, C_{H,H} = C_H$ ; otherwise the ratio  $c$  weakens the dependence by a factor increasing with the difference between  $\mathcal{H}$  values which accounts for the varying local amplitudes of different trajectory segments.

### 3. Stepwise changes of Hurst exponent and diffusion coefficient

The simplest—and essential—practical example for an evolving  $H$  concerns the switching between one distinct type of environment to another, and for which we can neglect the influence of short transition periods. In the model we then have that  $\mathcal{H}_t, \mathcal{D}_t$  reduce to step functions with values  $(H_1, D_1), (H_2, D_2)$ , etc., at fixed intervals. As in

<sup>+</sup> The process here is understood as a random generalised function, i.e., this definition uniquely determines all integrals  $\int \phi(t) dB_{\mathcal{H}}(t)$  for bounded  $\phi$  with bounded support.

any of the intervals with constant  $\mathcal{H}_t, \mathcal{D}_t$  the increments of IMFBM are—in isolation—equivalent to FBM increments, the corresponding pieces of trajectory are identical to segments of FBM with corresponding parameters  $H_j, D_j$ . If such a segment were measured without the rest of the trajectory the *increments* would be indistinguishable from those of normal FBM. Any statistical property, based on ensemble-averages, time-averages, or both, will be the same. When multiple such segments are experimentally observed, the IMFBM model provides additional information about their codependence on the level of the *position*. Namely, any two trajectory segments depend on each other through their compound Hurst exponents and diffusivities,  $(H_j + H_{j+1})/2$  and diffusivity  $c_{H_j, H_{j+1}} \sqrt{D_j D_{j+1}}$ . Additionally, the full memory structure of a trajectory  $B_{\mathcal{H}}$  for any number of transitions can be expressed by the direct formula obtained from the covariance integral (4), see equation (S3).

To better understand the behaviour of this model let us consider a simple concrete case crucial for many applications. A single transition between two pairs of values  $(H_i, D_i)$  at time  $\tau$  corresponds to the protocol

$$\mathcal{H}_t = \begin{cases} H_1, & t \leq \tau, \\ H_2, & t > \tau, \end{cases} \quad \mathcal{D}_t = \begin{cases} D_1, & t \leq \tau, \\ D_2, & t > \tau. \end{cases} \quad (7)$$

The associated MSD reads

$$\langle B_{\mathcal{H}}(t)^2 \rangle = \begin{cases} D_1 t^{2H_1}, & t \leq \tau, \\ D_2 (t - \tau)^{2H_2} + D_1 \tau^{2H_1} \\ + c_{H_1, H_2} \sqrt{D_1 D_2} (t^{H_1+H_2} - (t - \tau)^{H_1+H_2} - \tau^{H_1+H_2}), & t > \tau. \end{cases} \quad (8)$$

The cross term for  $t > \tau$  has the asymptotic  $\sim (H_1 + H_2) \tau c_{H_1, H_2} \sqrt{D_1 D_2} t^{H_1+H_2-1}$ . Thus, as expected, the MSD is dominated by  $H_2$  at long times,  $\langle B_{\mathcal{H}}(t)^2 \rangle \sim D_2 t^{2H_2}$ ,  $t \rightarrow \infty$ . When  $H_1 + H_2 < 1$  the cross term disappears completely at long times. In the opposite regime  $H_1 + H_2 > 1$  its remaining presence is indicative of the long memory in the system. Shortly after the transition at,  $t = \tau + \delta$  with  $\delta \rightarrow 0$ , the asymptotic expansion of the MSD reads

$$\langle B_{\mathcal{H}}(t)^2 \rangle \sim D_1 \tau^{2H_1} + D_2 \delta^{2H_2} + (H_1 + H_2) c_{H_1, H_2} \sqrt{D_1 D_2} \tau^{H_1+H_2-1} \delta - c_{H_1, H_2} \sqrt{D_1 D_2} \delta^{H_1+H_2}. \quad (9)$$

Among the three terms depending on  $\delta$  the one with the smallest exponent dominates at  $\delta \rightarrow 0$ .

Interestingly, in the case of weakening subdiffusion  $H_1 + H_2 < 1$ ,  $H_1 < H_2$ , or subdiffusion with decreasing diffusivity  $H_1 = H_2 < 1/2$ ,  $D_2 < D_1$ , after the transition at  $\tau$  the MSD locally decreases. This may at first be seen as a paradox, taking into account that displacements after time  $\tau$  do increase,  $\langle (B_{\mathcal{H}}(t + \tau) - B_{\mathcal{H}}(\tau))^2 \rangle = D_2 t^{2H_2}$ . However, a similar behaviour can also be observed for other models with time-dependent antipersistence and is caused by the fact that locally antipersistence dominates persistence,  $t^{2H_1} \ll t^{2H_2}$  for  $H_2 < H_1, t \rightarrow 0$ . Thus, the tendency to reverse



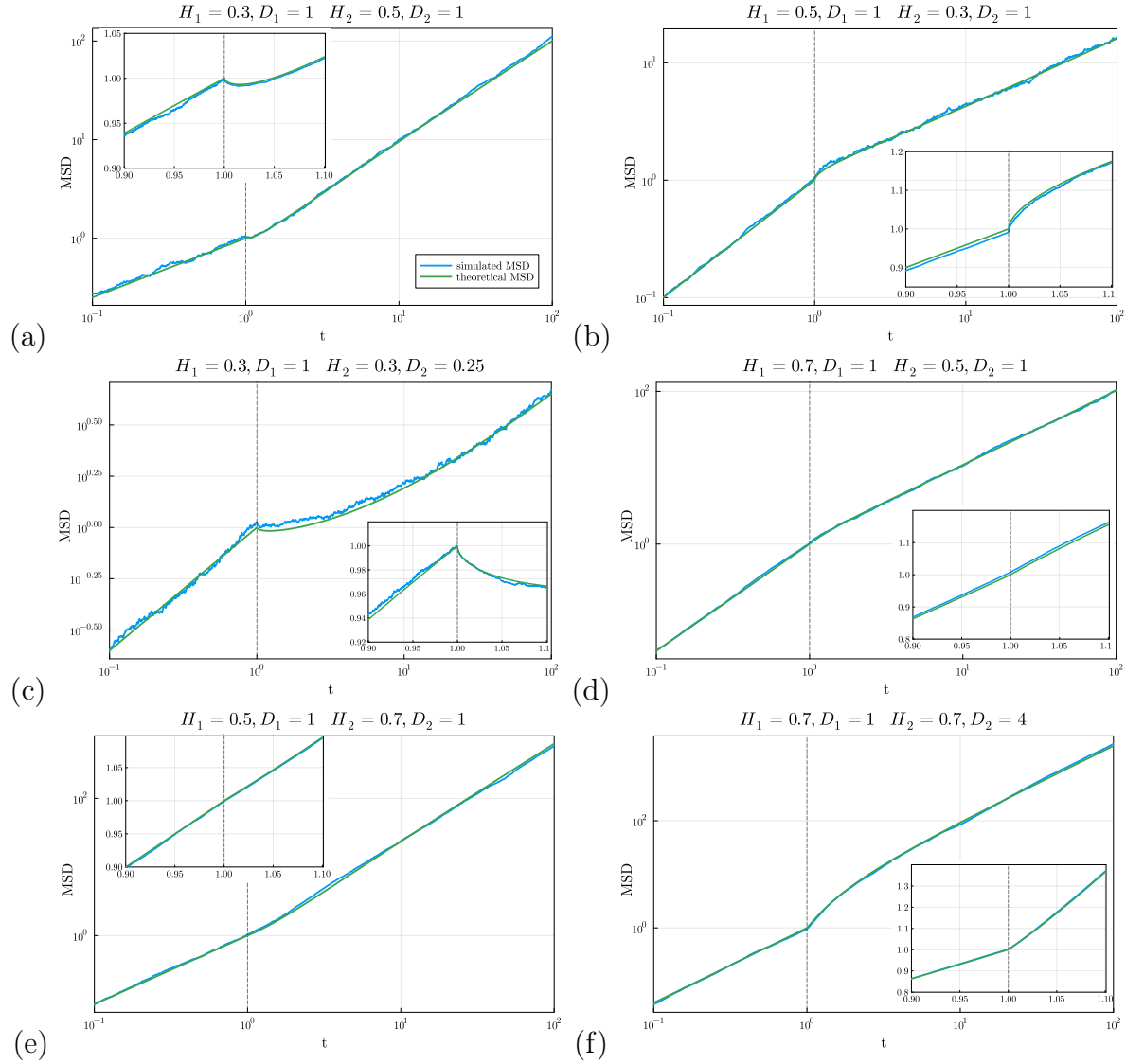


**Figure 4.** Illustration of different types of transitions at  $t = 1$ : (a) subdiffusion to normal diffusion, (b) normal to subdiffusion, (c) subdiffusion to subdiffusion with different diffusivity, (d) superdiffusion to normal diffusion, (e) normal diffusion to superdiffusion, and (f) superdiffusion to superdiffusion with different diffusivity. The MSDs in the main plots were estimated using  $10^3$  trajectories. In order to visualise details of the motion, in the inset plots with larger samples of  $10^5$  were used.

the progression wins until a new piece of trajectory accumulates sufficient weight. The same effect occurs for decreasing  $D$  as then new increments have less weight due to their smaller amplitudes. Different examples of Hurst exponent transitions are shown in figure 4.

#### 4. Discussion

The subject of anomalous diffusion is sometimes called a "jungle" of models which alludes to the richness and variety of mathematical tools it offers but also to common

	classical MFBMs	IMFBM
dependence	long memory	long memory
fractal dimension	$\begin{cases} 2 - H_1, & t < \tau \\ 2 - H_2, & t > \tau \end{cases}$	$\begin{cases} 2 - H_1, & t < \tau \\ 2 - H_2, & t > \tau \end{cases}$
MSD	$\begin{cases} Dt^{2H_1}, & t \leq \tau \\ Dt^{2H_2}, & t > \tau \end{cases}$	$\begin{cases} D_1 t^{2H_1}, & t \leq \tau \\ \sim D_1 \tau^{2H_1} + D_*(t - \tau)^{2H_*}, & t > \tau \end{cases}$
trajectories	discontinuous at $\tau$	continuous

**Table 1.** Comparison of typical already established MFBM models and IMFBM for one change of Hurst exponent at time  $\tau$ . In the line for MSD  $H_* \equiv \min\{H_2, 1/2, (H_1 + H_2)/2\}$  and constant  $D_*$  can be read from the full formula (8). Note that for different variants of MFBM the exact behaviour in the left column may differ, the features given are typical, see [65].

difficulties in deciphering the ones best suited to a given system. New methods of describing transient diffusion phenomena introduce additional time dependencies of the transport parameters which adds yet another layer to the already complex modelling problem. This is why it is crucial to have at disposal models as simple as possible, and which preserve as much as possible from the elegant symmetries of anomalous diffusion processes—this is what made them useful in the first place.

What is presented here is an attempt at introducing a time dependence into FBM while keeping its memory structure as simple as possible. Such processes—multifractional FBMs—have already been developed but they were not widely used for describing diffusion phenomena and existing models do not have probabilistic features which we would expect from those for physical and biological systems. The introduced IMFBM models a particle diffusing in a complex environment for which conditions change in time and after the transition new displacements are governed by new diffusivity and new Hurst exponent while also keeping the memory of its history before the transition; see table 1 for a comparison between classical MFBM models and IFBM.

It has two central features: the geometric averaging of diffusivities and arithmetic averaging of Hurst exponents (see (3)) which are fully experimentally verifiable and distinguish it from other MFBM models.

IMFBM is a generalisation of both FBM and scaled Brownian motion used to model diffusion with changing diffusivity. The transitions of  $H$  and  $D$  can be both smooth or discontinuous. It is Gaussian. The associated MSD and covariance can always be expressed as integrals which for the crucial case of step step function protocols for  $H$  and  $D$  reduce to elementary functions. The local fractal dimension of the IMFBM trajectories is  $2 - \mathcal{H}_t$ .

Mathematical models such as IMFBM are indispensable in creating objective tools to determine the best combination of stochastic models and their parameters given measured data. They are becoming increasingly important with the fast growing numbers of increasingly refined experiments in complex systems. Some of the existing

solutions are provided, e.g., by Bayesian analyses [84, 85] or the machine learning apparatus [20, 86–88]. We provide a guide towards statistical estimation of the transport parameters in our IMFBM model in the Supplementary Material.

The IMFBM process can be used to model the data directly but we also see a potential value in using it to construct more sophisticated tools. In many systems the evolution of  $H$  and  $D$  should be considered to be random itself. This is an example of a doubly stochastic modelling approach which is straightforward to introduce into anomalous diffusion studies using IMFBM. Another classical and indispensable tool in stochastic modelling are Langevin equations which are a class of stochastic differential equations suited to describe the diffusion phenomena. It seems very natural to use IMFBM as a noise in those equations which would then allow us to study the stochastic motion in the presence of an external potential and which fulfils local fluctuation-dissipation relations.

## Acknowledgments

RM was supported by the German Ministry for Education and Research (BMBF, grant STAXS).

## References

- [1] Einstein A 1905 *Ann. der Physik* **322** 549–560
- [2] von Smoluchowski M 1906 *Ann. der Physik* **326** 756–780
- [3] Sutherland W 1905 *Philos. Mag.* **9** 781–785
- [4] Lemons D and Gythiel A 1997 *Am. J. Phys.* **65** 1079–1081
- [5] Wiener N 1921 *Proc. Natl. Acad. Sci. U.S.A.* **7** 294–298
- [6] Brenig W 1989 *Statistical Theory of Heat: Nonequilibrium Phenomena* (Berlin, Heidelberg: Springer)
- [7] Lifshitz E M and Pitaevski L P 1981 *Landau and Lifshitz Course of Theoretical Physics 10: Physical Kinetics* (Oxford UK: Butterworth-Heinemann)
- [8] Krapivsky P, Redner S and Ben-Naim E 2010 *A Kinetic View of Statistical Physics* (Cambridge, UK: Cambridge University Press)
- [9] Livi R and Politi P 2017 *Nonequilibrium Statistical Physics: A Modern Perspective* (Cambridge, UK: Cambridge University Press)
- [10] van Kampen N 1981 *Stochastic processes in physics and chemistry* (Amsterdam: North Holland)
- [11] Coffey W and Kalmykov Y 2012 *The Langevin equation* (Singapore: World Scientific)
- [12] Perrin J 1908 *Compt. Rend. (Paris)* **146** 967
- [13] Norlund I 1914 *Z. Phys. Chem.* **87** 40
- [14] Manzo C and Garcia-Parajo M F 2015 *Rep. Prog. Phys.* **78** 124601
- [15] Vilks O, Aghion E, Avgar T, Beta C, Nagel O, Sabri A, Sarfati R, Schwartz D K, Weiss M, Krapf D, Nathan R, Metzler R and Assaf M 2022 *Phys. Rev. Res.* **4**(3) 033055
- [16] Metzler R, Jeon J H, Cherstvy A G and Barkai E 2014 *Phys. Chem. Chem. Phys.* **16** 24128–24164
- [17] Sokolov I M 2012 *Soft Matter* **8** 9043–9052
- [18] Barkai E, Garini Y and Metzler R 2012 *Phys. Today* **65**(8) 29
- [19] Krapf D and Metzler R 2019 *Phys. Today* **72** 48–54
- [20] Muñoz-Gil G, Volpe G, Garcia-March M A, Aghion E, Argun A, Hong C B, Bland T, Bo S, Conejero J A, Firbas N, Garibo I Orts Ò, Gentili A, Huang Z, Jeon J H, Kabbech H, Kim

- Y, Kowalek P, Krapf D, Loch-Olszewska H, Lomholt M A, Masson J B, Meyer P G, Park S, Requena B, Smal I, Song T, Szwabiński J, Thapa S, Verdier H, Volpe G, Widera A, Lewenstein M, Metzler R and Manzo C 2021 *Nat. Commun.* **12** 6253
- [21] Metzler R and Klafter J 2000 *Phys. Rep.* **339** 1–77
- [22] Meerson B, Bénichou O and Oshanin G 2022 *Phys. Rev. E* **106**(6) L062102
- [23] Kolmogorov A N 1940 *C.R. (Doklady) Acad. Sci. URSS (NS)* **26** 115–118
- [24] Mandelbrot B B and Ness J W V 1968 *SIAM Rev.* **10**(4) 422–437
- [25] Graves T, Gramacy R, Watkins N and Franzke C 2017 *Entropy* **19** 437
- [26] Hurst H E 1951 *Trans. Am. Soc. Civ. Eng.* **116** 770–799
- [27] Mikosch T, Resnick S, Rootzén H and Stegeman A 2002 *Ann. Appl. Probab.* **12** 23 – 68
- [28] Lomax O, Bates M L and Whitworth A P 2018 *Mon. Not. R. Astron. Soc.* **480** 371–380
- [29] Gatheral J, Jaisson T and Rosenbaum M 2014 *SSRN Electron. J.*
- [30] Jeon J H, Tejedor V, Burov S, Barkai E, Selhuber-Unkel C, Berg-Sørensen K, Oddershede L and Metzler R 2011 *Phys. Rev. Lett.* **106** 048103
- [31] Jeon J H, Leijne N, Oddershede L B and Metzler R 2013 *New J. Phys.* **15** 045011
- [32] Weber S C, Spakowitz A J and Theriot J A 2010 *Phys. Rev. Lett.* **104**(23) 238102
- [33] Szymanski J and Weiss M 2009 *Phys. Rev. Lett.* **103** 038102
- [34] Weiss M 2013 *Phys. Rev. E* **88**(1) 010101
- [35] Jeon J H, Monne H M S, Javanainen M and Metzler R 2012 *Phys. Rev. Lett.* **109** 188103
- [36] Krapf D, Lukat N, Marinari E, Metzler R, Oshanin G, Selhuber-Unkel C, Squarcini A, Stadler L, Weiss M and Xu X 2019 *Phys. Rev. X* **9**(1) 011019
- [37] Reverey J F, Jeon J H, Bao H, Leippe M, Metzler R and Selhuber-Unkel C 2015 *Sci. Rep.* **5** 1–14
- [38] Thapa S, Lukat N, Selhuber-Unkel C, Cherstvy A G and Metzler R 2019 *J. Chem. Phys.* **150** 144901
- [39] Vilk O, Aghion E, Nathan R, Toledo S, Metzler R and Assaf M 2022 *J. Phys. A* **55** 334004
- [40] Lampo T J, Stylianidou S, Backlund M P, Wiggins P A and Spakowitz A J 2017 *Biophys. J.* **112** 532–542
- [41] Sabri A, Xu X, Krapf D and Weiss M 2020 *Phys. Rev. Lett.* **125**(5) 058101
- [42] Jeon J H, Javanainen M, Martinez-Seara H, Metzler R and Vattulainen I 2016 *Phys. Rev. X* **6** 021006
- [43] Wang W, Cherstvy A G, Chechkin A V, Thapa S, Seno F, Liu X and Metzler R 2020 *J. Phys. A* **53** 474001
- [44] Wang W, Seno F, Sokolov I M, Chechkin A V and Metzler R 2020 *New J. Phys.* **22** 083041
- [45] Balcarek M, Burnecki K, Thapa S, Wyłomańska A and Chechkin A 2022 *Chaos* **32** 093114
- [46] Korabel N, Clemente G D, Han D, Feldman F, Millard T H and Waigh T A 2022 *Comm. Phys.* **5** 269
- [47] Bouchaud J P and Georges A 1990 *Phys. Rep.* **195** 127–293
- [48] Beran J 1994 *Statistics for Long-Memory Processes* (New York: Chapman & Hall)
- [49] Lutz E 2001 *Phys. Rev. E* **64**(5) 051106
- [50] Kou S C and Xie X S 2004 *Phys. Rev. Lett.* **93**(18) 180603
- [51] Ślęzak J, Metzler R and Magdziarz M 2018 *New J. Phys.* **20** 023026
- [52] Picard J 2011 *Representation Formulae for the Fractional Brownian Motion* (Berlin, Heidelberg: Springer) pp 3–70
- [53] Odermatt P D, Miettinen T P, Lemièrre J, Kang J H, Bostan E, Manalis S R, Huang K C and Chang F 2021 *eLife* **10** e64901
- [54] Barlow A J, Harrison G, Irving J B, Kim M G, Lamb J and Pursley W C 1972 *Proc. R. Soc. Lond.* **327** 403–412
- [55] Caspers J, Ditz N, Krishna Kumar K, Ginot F, Bechinger C, Fuchs M and Küger M 2023 *J. Chem. Phys.* **158** 024901
- [56] Levin M, Bel G and Roichman Y 2021 *J. Chem. Phys.* **154** 144901
- [57] 2001 *Science* **294** 1929–1932

- [58] Meyer P G, Cherstvy A G, Seckler H, Hering R, Blaum N, Jeltsch F and Metzler R 2023 *E-print arXiv:2305.06601*
- [59] Etoc F, Balloul E, Vicario C, Normanno D, Liße D, Sittner A, Piehler J, Dahan M and Coppey M 2018 *Nat. Mater.* **17** 740–746
- [60] Heller I, Sitters G, Broekmans O D, Farge G, Menges C, Wende W, Hell S W, Peterman E J G and Wuite G J L 2013 *Nat. Methods* **10** 910–916
- [61] Peltier R F and Véhel J L 1995 [*Research Report*] RR-2645, INRIA. 1995. *ffinria-00074045f*
- [62] Benassi A, Cohen S and Istas J 1998 *Stat. Probab. Lett.* **39** 337–345
- [63] Benassi A, Roux D and Jaffard S 1997 *Rev. Mat. Iberoam* **13** 19–90
- [64] Ayache A, Cohen S and Véhel J L 2000 The covariance structure of multifractional Brownian motion, with application to long range dependence 2000 *IEEE International Conference on Acoustics, Speech, and Signal Processing. Proceedings (Cat. No. 00CH37100)* vol 6 (IEEE) pp 3810–3813
- [65] Stoev S A and Taqqu M S 2006 *Stoch. Process. Their Appl.* **116** 200–221
- [66] Wang W, Balcerek M, Burnecki K, Chechkin A V, Janusonis S, Ślęzak J, Vojta T, Wyłomańska A and Metzler R 2023
- [67] Ray B K and Tsay R S 2002 *J. Time Ser. Anal.* **23** 687–705
- [68] Corlay S, Lebovits J and Véhel J L 2014 *Math. Finance* **24** 364–402
- [69] Bianchi S, Pantanella A and Pianese A 2013 *Quant. Finance* **13** 1317–1330
- [70] Peng Q and Zhao R 2018 *Chaos Solit. Fractals* **115** 248–267
- [71] Wu P, Muzy J F and Bacry E 2022 *Phys. A: Stat. Mech. Appl.* **604** 127919
- [72] Bianchi G, Vieira F and Ling L L 2004 A novel network traffic predictor based on multifractal traffic characteristic *IEEE Global Telecommunications Conference, 2004. GLOBECOM '04.* vol 2 pp 680–684 Vol.2
- [73] Echelard A, Véhel J L and Barrière O 2010 Terrain modeling with multifractional Brownian motion and self-regulating processes *Computer Vision and Graphics* ed Bolc L, Tadeusiewicz R, Chmielewski L J and Wojciechowski K (Berlin, Heidelberg: Springer) pp 342–351
- [74] Lee K C 2013 *Nonlinear Process. Geophys.* **20**
- [75] Wang Y, Cavanaugh J E and Song C 2001 *J. Stat. Plan. Inference* **99** 91–110
- [76] Balcerek M and Burnecki K 2020 *Entropy* **22**
- [77] Szarek D, Jabłoński I, Krapf D and Wyłomańska A 2022 *Chaos* **32** 083148
- [78] Lévy P 1953 *Random functions: general theory with special reference to Laplacian random functions* (Berkeley: University of California Press)
- [79] Jeon J H, Chechkin A V and Metzler R 2014 *Phys. Chem. Chem. Phys.* **16**(30) 15811–15817
- [80] Lim S C and Muniandy S V 2002 *Phys. Rev. E* **66**(2) 021114
- [81] Benassi A, Cohen S and Istas J 2003 *C. R. Math.* **336** 267–272
- [82] Falconer K 1990 *Fractal geometry* (Chichester, UK: John Wiley & Sons)
- [83] Priestley M B 1965 *J. R. Stat. Soc. Ser. B Methodol.* **27** 204–237
- [84] Thapa S, Lomholt M A, Krog J, Cherstvy A G and Metzler R 2018 *Phys. Chem. Chem. Phys.* **20**(46) 29018–29037
- [85] Robson A, Burrage K and Leake M C 2013 *Philos. Trans. R. Soc. Lond. B Biol. Sci.* **368** 20120029
- [86] Seckler H and Metzler R 2022 *Nat. Commun.* **13** 6717
- [87] Manzo C, noz Gil G M, Volpe G, Garcia-March M A, Lewenstein M and Metzler R 2023 *J. Phys. A* **56** 010401
- [88] Kowalek P, Loch-Olszewska H, Łaszczuk Ł, Opała J and Szwabiński J 2022 *J. Phys. A* **55** 244005
- [89] Kroese D, Taimre T and Botev Z 2013 *Handbook of Monte Carlo Methods* (Hoboken, NJ: Wiley)
- [90] Coeurjolly J F 2000 *J. Stat. Softw.* **5** 1–53

# Minimal model of diffusion with time changing Hurst exponent

## Supplementary material

Jakub Ślęzak<sup>†</sup> and Ralf Metzler<sup>‡,‡</sup>

<sup>†</sup> Hugo Steinhaus Center, Wrocław University of Science and Technology, Poland

<sup>‡</sup> Institute of Physics & Astronomy, University of Potsdam, Germany

<sup>‡</sup> Asia Pacific Centre for Theoretical Physics, Pohang 37673, Republic of Korea

### 1. Simulation

We divide simulation methods of the IMFBM into two cases: the situation when the covariance of  $B_{\mathcal{H}}$  can be efficiently calculated and when it cannot. Let us start from the former case.

The stochastic integral (6) which represents  $dB_{\mathcal{H}}$  and its covariance (3) are singular because they are defined in the limit of infinitesimal  $dt$ . This singularity can be removed if one takes one step back and approximates this process at small but fixed  $\Delta t$ . Repeating the derivation of IMFBM, finite differences of FBM from equation (2) lead to the numerator  $e^{i\omega(t+\Delta t)} - e^{i\omega t}$  instead of the limiting form  $i\omega e^{i\omega t}$ . Substituting  $D \rightarrow \mathcal{D}_t, H \rightarrow \mathcal{H}_t$  yields

$$\Delta \tilde{B}_{\mathcal{H}}(t) \equiv \frac{\sqrt{\mathcal{D}_t}}{\gamma_{\mathcal{H}_t}} \int_{-\infty}^{\infty} \frac{e^{i\omega\Delta t} - 1}{|\omega|^{\mathcal{H}_t+1/2}} e^{i\omega t} dZ(\omega). \quad (\text{S1})$$

For this process the  $\propto \omega$ -dependence of the numerator at  $\omega \rightarrow 0$  cancels the singularity of the denominator and allows for a stable simulation. Given this process, it can then be used to generate  $\Delta \tilde{B}_{\mathcal{H}}(t)$ . Then one can calculate  $\tilde{B}_{\mathcal{H}}(n\Delta t) \equiv \sum_{k=1}^n \Delta \tilde{B}_{\mathcal{H}}(k\Delta t)$ . This process approximates  $B_{\mathcal{H}}$  as  $\Delta t \rightarrow 0$ .

The integral (S1) can be approximated directly by Riemann summation over a finite sequence of iid  $\mathcal{N}(0, \Delta\omega)$  variables  $\Delta Z(\omega)$ , preferably probing different  $\omega$  at logarithmic spans in order to better catch the power-law distributed probabilistic mass. Alternatively, the process  $\Delta \tilde{B}_{\mathcal{H}}$  has the covariance

$$\langle \Delta \tilde{B}_{\mathcal{H}}(s) \Delta \tilde{B}_{\mathcal{H}}(t) \rangle = \frac{1}{2} c_{\mathcal{H}_s, \mathcal{H}_t} \sqrt{D_s D_t} \cdot (|t - s + \Delta t|^{\mathcal{H}_s + \mathcal{H}_t} + |t - s - \Delta t|^{\mathcal{H}_s + \mathcal{H}_t} - 2|t - s|^{\mathcal{H}_s + \mathcal{H}_t}). \quad (\text{S2})$$

Given this formula, its realisations can be simulated exactly using the Cholesky decomposition method [89].

For a given interval  $a \leq t \leq b$  containing  $n$   $\Delta t$ -spaced points we first need to store the covariance matrix  $\Sigma_{i,j} \equiv \langle \Delta \tilde{B}_{\mathcal{H}}(a + i\Delta t) \Delta \tilde{B}_{\mathcal{H}}(a + j\Delta t) \rangle$  which takes  $\mathcal{O}(n^2)$  memory space. Using one of the standard Cholesky decomposition algorithms we calculate the lower triangular matrix  $L$  such that  $\Sigma = LL^\dagger$ . These algorithms use  $\mathcal{O}(n^3)$  time. Finally, applying this matrix to the vector of iid  $\mathcal{N}(0, 1)$  variables returns one realisation of  $\Delta \tilde{B}_{\mathcal{H}}$ . This method is initially memory and time consuming with respect to  $n$  but then generating new realisations is very fast. One also needs to be careful simulating samples with low local  $\mathcal{H}_t$ , around 0.1, because the dependence between increments is then chaotic and for longer times may be dominated by the numerical errors of the Cholesky decomposition, leading to false normal diffusion. This regime of very low Hurst exponents is however rarely met in practice.

In the former category of simulations, when the covariance of  $B_{\mathcal{H}}$  can be effectively determined, it is better to generate samples of  $B_{\mathcal{H}}$  directly, without  $\Delta \tilde{B}_{\mathcal{H}}(t)$ . This can be done again by the Cholesky decomposition and for any choice of sampling times  $t_1, t_2, \dots, t_n$ , not necessarily equally spaced. The covariance of  $B_{\mathcal{H}}$  can be numerically approximated using an integral of type (4), but one then needs to be careful, because, as a result of errors, the resulting matrix  $\Sigma$  may not be exactly positive semidefinite, a requirement for the Cholesky decomposition. Additional regularisation may be required beforehand.

A perfect situation occurs when the covariance integral (4) can be calculated analytically. This is the case for any stepwise protocol of constant  $(H_j, D_j)$  on intervals  $(\tau_{j-1}, \tau_j)$ . Without any loss of generality we can assume that  $s = \tau_n$  and  $t = \tau_m$  (by taking  $H_{n-1} = H_n, D_{n-1} = D_n$ ) which allows us to formulate the result in an elegant manner,

$$\langle B_{\mathcal{H}}(s)B_{\mathcal{H}}(t) \rangle = \sum_{j=1}^n \sum_{k=1}^m A_{j,k} (|\tau_j - \tau_{k-1}|^{H_j+H_k} + |\tau_{j-1} - \tau_k|^{H_j+H_k} - |\tau_{j-1} - \tau_{k-1}|^{H_j+H_k} - |\tau_j - \tau_k|^{H_j+H_k}), \quad (\text{S3})$$

where we denoted  $A_{j,k} \equiv c_{H_j, H_k} \sqrt{D_j D_k} / 2$ . In particular for the case of only a single change of parameters at time  $\tau$  the above formula produces

$$\langle B_{\mathcal{H}}(s)B_{\mathcal{H}}(t) \rangle = \begin{cases} D_1(t^{2H_1} + s^{2H_2} - |t-s|^{2H_1}), & s \leq t \leq \tau \\ \frac{1}{2} \left\{ \begin{aligned} & D_1(s^{2H_1} + \tau^{2H_1} - |\tau-s|^{2H_1}) + \\ & c_{H_1, H_2} \sqrt{D_1 D_2} (|\tau-s|^{H_1+H_2} + t^{H_1+H_2} - \tau^{H_1+H_2} - |t-s|^{H_1+H_2}), \\ & 2D_2 \tau^{2H_1} + \end{aligned} \right. & s < \tau < t \\ \frac{1}{2} \left\{ \begin{aligned} & c_{H_1, H_2} \sqrt{D_1 D_2} (s^{H_1+H_2} + t^{H_1+H_2} - 2\tau^{H_1+H_2} - |t-\tau|^{H_1+H_2} - |s-\tau|^{H_1+H_2}) + \\ & D_2 (|s-\tau|^{2H_2} + |t-\tau|^{2H_2} - |t-s|^{2H_2}), \end{aligned} \right. & \tau \leq s \leq t. \end{cases} \quad (\text{S4})$$

One last point we have to make about the numerical approach to IMFBM is that the memoryless case  $(\mathcal{H}_s + \mathcal{H}_t)/2 = 1/2$  is singular in the same way as for simulations of classical FBM. Most of the methods which explicitly use the kernel  $|t-s|^{\mathcal{H}_s + \mathcal{H}_t - 2}$  will result in numerical errors. One needs to consider only "perturbed memorylessness"  $(\mathcal{H}_s + \mathcal{H}_t)/2 = 1/2 + \epsilon$ , or, preferably whenever possible, implement this case separately, by simulating independent increments [90].

A computer code for IMFBM simulation is provided in in the GitHub repository <https://github.com/jaksle/IMFBM>.

## 2. Estimation

We provide two estimation methods for IMFBM which have different requirements and complement each other. They are designed for experimental data measured at constant rate,  $X_j = B_{\mathcal{H}}(\Delta t j)$ ,  $j \in \{0, 1, 2, \dots, N\}$ . We denote the corresponding increments by  $\Delta X_j \equiv X_{j+1} - X_j$ .

In the first case we discuss a method which is of use even if only one trajectory is available and which can detect variability of subdiffusive/normal  $H, D$ . For stepwise changes it estimates their local values and transition moments. It is based on the second variation and lag 1 covariation of the time series,

$$\mathcal{V}_k \equiv \sum_{i=0}^k (\Delta X_i)^2, \quad \mathcal{C}_j \equiv \sum_{i=0}^k \Delta X_i \Delta X_{i+1}. \quad (\text{S5})$$

Due to the law of large numbers, for big  $k$ ,  $\mathcal{V}_k$  is asymptotically dominated by a straight line with slope equal to the variance of the series increments  $\mathcal{V}_k = \sigma^2 k + \mathcal{O}(\sqrt{k})$ ,  $\sigma^2 \equiv \langle (\Delta X_i)^2 \rangle$ , similarly with a covariance with slope equal to the lag 1 covariance which we separate into variance and correlation factors  $\mathcal{C}_k = \sigma^2 \rho k + \mathcal{O}(\sqrt{k})$ ,  $\rho \equiv \langle \Delta X_i \Delta X_{i+1} \rangle / \langle (\Delta X_i)^2 \rangle$ . Thus, fitting a linear function to these quantities yields the estimates  $\sigma_{\text{est}}^2$  and  $\rho_{\text{est}}$ .

In the final step, the Hurst exponent is reconstructed from the correlation  $\rho_{\text{est}}$ . The covariance formula (3) is valid for infinitely small increments, for finite sampling frequency a correction should be included, resulting in the relation  $\rho = 2^{2H} - 2$  and  $H_{\text{est}} = \log_2(2\rho_{\text{est}} + 2)/2$ . Given the estimate  $H_{\text{est}}$  the diffusivity is  $D_{\text{est}} = \sigma_{\text{est}}^2 / (\Delta t)^{2H_{\text{est}}}$ .

At transition moments of  $H$  or  $D$ , the slopes of  $\mathcal{V}$  and  $\mathcal{C}$  change as well and they become polygonal chains; this is caused by the fact that IMFBM is locally undistinguishable from FBM, and slope is a

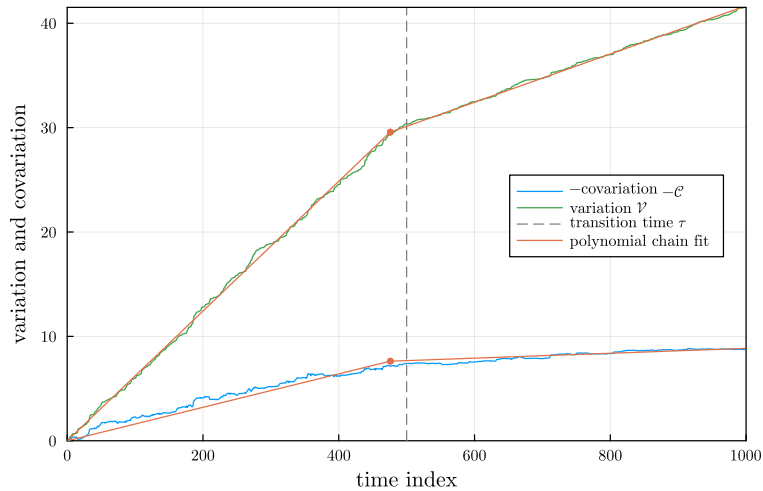


**Figure S1.** Estimation for a single trajectory of length 1000. For better visual presentation minus the covariation is shown. The obtained estimate for the transition time is  $\tau_{\text{est}}=476$ , comparing nicely with the true value 500. From the slopes of the fitted polynomial chain we obtained estimates of the Hurst exponents and diffusivities  $H_{1,\text{est}} = 0.28, D_{1,\text{est}} = 0.86, H_{2,\text{est}} = 0.42, D_{2,\text{est}} = 1.13$ .

	$H_1$	$D_1$	$\tau$	$H_2$	$D_2$
$n = 500$	$0.29 \pm 0.06$	$1.0 \pm 0.5$	$244 \pm 30$	$0.44 \pm 0.06$	$1.6 \pm 0.7$
$n = 1000$	$0.29 \pm 0.04$	$1.0 \pm 0.4$	$494 \pm 32$	$0.44 \pm 0.05$	$1.6 \pm 0.7$
$n = 10000$	$0.30 \pm 0.01$	$1.0 \pm 0.2$	$5001 \pm 63$	$0.45 \pm 0.02$	$1.5 \pm 0.5$

**Table S1.** Means and mean squared deviations of the IMFBM estimators for trajectories with different lengths  $n$ . The switching times were chosen at the midpoint of each trajectory.

local property. The estimation procedure is then as follows: plot  $\mathcal{V}, \mathcal{C}$  and assess if their slope changes; this suggests an IMFBM transition. Fit a polygonal chain to  $\mathcal{V}$  and  $\mathcal{C}$  using, e.g., the ordinary least squares method. Read the transition moments and evaluate estimates of the local Hurst exponent and the diffusivity from the slopes of the chain segments.

We tested this method using trajectories of IMFBM at  $0 < t < 10$ , which change from  $H_1 = 0.3, D_1 = 1$  to  $H_2 = 0.45, D_2 = 1.5$  in the middle. One exemplary estimation is visualised in figure S1. Using a sample of 1000 realisations of IMFBM we measured the behaviour of the estimators for different lengths of trajectories. The results are listed in Table S1 which proves that this method allows for reliable estimation using a very moderate amount of data.

The limitations of this method are twofold. First, it does not work for superdiffusion for which due to the long memory variation and covariation are not linear. Second, it is sensitive to high frequency data distortions due to using only a lag 1 correlation. For example, additive noise would distort the estimation of the Hurst exponent by weakening the short range correlation; however, the transition moment would still be correctly detected which then opens the possibility to use classical statistical methods for FBM at each detected segment. The method can also be generalised to use correlations at different lags.

The second method uses a sample of trajectories which share  $\mathcal{H}$  and  $\mathcal{D}$ , or at least we want to estimate some form of effective, averaged  $\mathcal{H}$  and  $\mathcal{D}$  from the sample. Conceptually this method is very straightforward: given a sample we estimate the local MSD, fit it with a power law and from this obtain



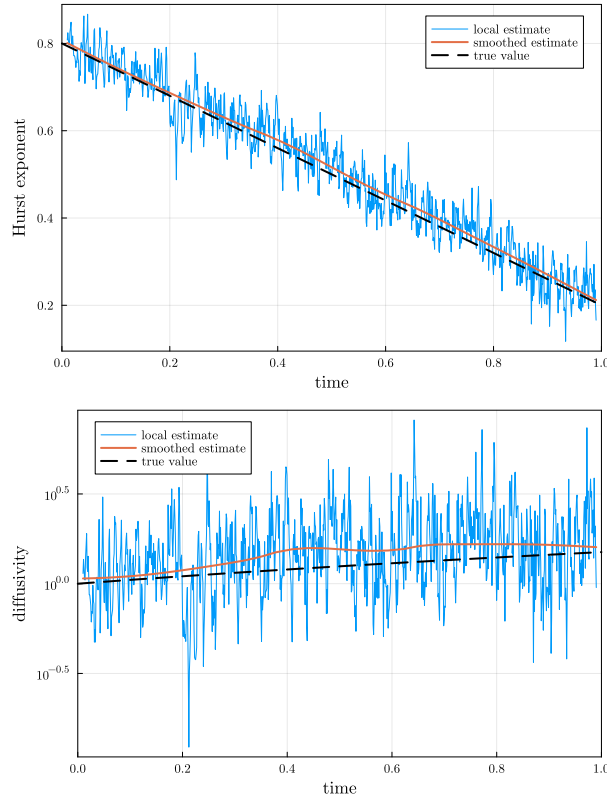


**Figure S2.** Estimation based on a sample of 100 trajectories with lengths 1000 each. The Hurst index was decreasing linearly from 0.8 to 0.2, the diffusivity was increasing linearly from 1 to 1.5. The estimation window was  $w = 10$ . A smoothed estimate was obtained using the Loess method. Because of the multiplicative nature of the  $D$  estimation errors smoothing and data visualisation were performed in the  $\log y$  scale. Mean squared deviations of local estimates were  $\pm 0.04$  for  $H$  and  $\pm 0.5$  for  $\log D$ . Mean errors were 0.01 and 0.15, respectively.

local estimates of the Hurst exponent and diffusivity.

By "local MSD" we mean the quantity  $\delta_{s,t}^2 \equiv \langle (X_{s+t} - X_s)^2 \rangle$  which is also considered in literature under the names "structure function" or "semivariogram". For IMFBM, if  $H$  and  $D$  are constant in the interval  $(s, s+t)$  and equal to  $\mathcal{H}_s, \mathcal{D}_s$  the local MSD reads  $\delta_{s,t}^2 = \mathcal{D}_s t^{2\mathcal{H}_s}$ . It can be estimated as sample average  $\overline{(X_{j+k} - X_j)^2}$  and fitted as function of  $k \in \{0, 1, 2, \dots, w\}$  locally in a window  $w$ . The reliability of the estimation requires that  $\mathcal{H}, \mathcal{D}$  do not vary too much over this window. Choosing a proper  $w$  requires balancing the expected variability of the parameters and the MSD power law fit quality. We show an exemplary estimation in figure S2.

Computer code examples of IMFBM estimation are provided in the GitHub repository <https://github.com/jaksle/IMFBM>.